Report

Immunity

The Pore-Forming Protein Gasdermin D Regulates Interleukin-1 Secretion from Living Macrophages

Graphical Abstract

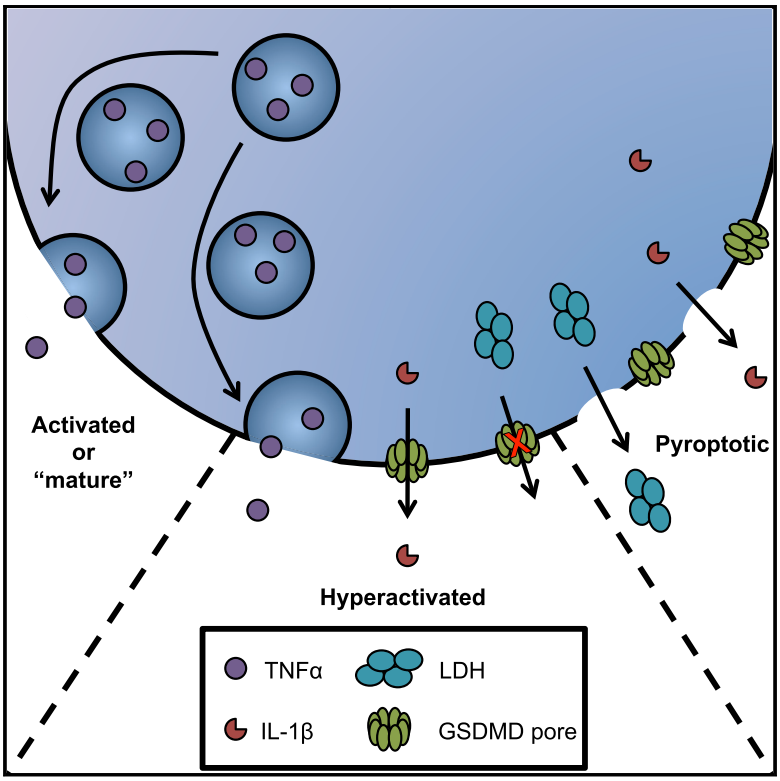

Authors

Charles L. Evavold, Jianbin Ruan, Yunhao Tan, Shiyu Xia, Hao Wu, Jonathan C. Kagan

Correspondence

jonathan.kagan@childrens.harvard.edu

In Brief

Inflammasomes elicit pyroptosis or cell hyperactivation, with the latter defined as living cells that release IL-1. Evavold et al report that the pore-forming protein gasdermin D regulates IL-1 release from hyperactive macrophages. Cell- and liposome-based assays revealed that gasdermin D pores permit IL-1 passage across intact lipid bilayers.

Highlights

- Multiple microbial and self-derived stimuli induce IL-1 release from living macrophages
- Inflammasomes can be detected within cells that display multiple signs of viability
- Living macrophages require gasdermin D to induce pore formation and IL-1 release
- Gasdermin D pores facilitate the release of IL-1 from liposomes and intact cells

Evavold et al., 2018, Immunity *48*, 35–44
January 16, 2018
https://doi.org/10.1016/j.immuni.2017.11.013

CellPress

Immunity
Report

The Pore-Forming Protein Gasdermin D Regulates Interleukin-1 Secretion from Living Macrophages

Charles L. Evavold,[1,2] Jianbin Ruan,[3] Yunhao Tan,[1] Shiyu Xia,[3] Hao Wu,[3] and Jonathan C. Kagan[1,2,4,*]
[1]Harvard Medical School and Division of Gastroenterology, Boston Children's Hospital, Boston, MA, USA
[2]Program in Immunology, Harvard Medical School, Boston, MA, USA
[3]Department of Biological Chemistry and Molecular Pharmacology, Harvard Medical School, and Program in Cellular and Molecular Medicine, Boston Children's Hospital, Boston, MA, USA
[4]Lead Contact
*Correspondence: jonathan.kagan@childrens.harvard.edu
https://doi.org/10.1016/j.immuni.2017.11.013

SUMMARY

The interleukin-1 (IL-1) family cytokines are cytosolic proteins that exhibit inflammatory activity upon release into the extracellular space. These factors are released following various cell death processes, with pyroptosis being a common mechanism. Recently, it was recognized that phagocytes can achieve a state of hyperactivation, which is defined by their ability to secrete IL-1 while retaining viability, yet it is unclear how IL-1 can be secreted from living cells. Herein, we report that the pyroptosis regulator gasdermin D (GSDMD) was necessary for IL-1β secretion from living macrophages that have been exposed to inflammasome activators, such as bacteria and their products or host-derived oxidized lipids. Cell- and liposome-based assays demonstrated that GSDMD pores were required for IL-1β transport across an intact lipid bilayer. These findings identify a non-pyroptotic function for GSDMD, and raise the possibility that GSDMD pores represent conduits for the secretion of cytosolic cytokines under conditions of cell hyperactivation.

INTRODUCTION

Interleukin-1 (IL-1) family cytokines induce inflammatory responses in numerous tissues of the body. These pyrogens are produced as cytosolic factors that lack an N-terminal secretion signal, and are therefore not released from cells via the conventional secretory pathway (Garlanda et al., 2013). Whereas the inflammatory functions of extracellular IL-1 are well-defined, the mechanisms by which these cytokines are released from cells remain elusive.

Central to the function of IL-1 are inflammasomes (Martinon et al., 2002), which are supramolecular organizing centers (SMOCs) that assemble in the cytosol in response to infection, ionic imbalance, and mitochondrial dysfunction (Latz et al., 2013; Kagan et al., 2014; Martinon et al., 2009). Inflammasomes consist of a sensor protein, an adaptor protein, and an inflammatory caspase effector protein (e.g., caspase-1). Caspase-1 is capable of cleaving IL-1 family cytokines that are translated in a pro-form, such as IL-1β and IL-18 (Cerretti et al., 1992; Garlanda et al., 2013). Cleavage of these factors is necessary for inflammatory activity.

Caspase-1 (and caspase-11) also cleave the cytosolic protein gasdermin D (GSDMD) (Kayagaki et al., 2015; Shi et al., 2015). Upon cleavage, the N-terminal fragment of GSDMD oligomerizes into ring-shaped structures in membranes (Aglietti et al., 2016; Ding et al., 2016; Liu et al., 2016; Sborgi et al., 2016). GSDMD rings form a pore in the plasma membrane that ultimately cause cell lysis. This cell death process (pyroptosis) is a highly inflammatory event, and provides a mechanism of IL-1 release (Kayagaki et al., 2015; Shi et al., 2015).

Pyroptosis is not the only means by which IL-1 is released from cells. For example, a set of oxidized lipids (oxPAPC) derived from dead mammalian cells induces inflammasome-dependent release of IL-1, but not cell death (Zanoni et al., 2016). The *N*-acetyl glucosamine (NAG) fragment of bacterial peptidoglycan (PGN) induces inflammasome-mediated IL-1 release from living macrophages (Wolf et al., 2016). Bacterial lipopolysaccharides (LPS) induce inflammasome-mediated release of IL-1 from living human monocytes (Gaidt et al., 2016), and living neutrophils also release IL-1 (Chen et al., 2014).

Viable cells that release inflammatory cytokines via the secretory pathway are known as "activated" or "mature" cells (Mellman et al., 1998), whereas dead cells that release IL-1 are considered "pyroptotic" (Kovacs and Miao, 2017). Viable cells that release IL-1 along with other cytokines exist in a state that differs from their activated or pyroptotic counterparts. This distinct activation state has been termed "hyperactive" (Zanoni et al., 2016). The recognition that phagocytes can release IL-1 while maintaining viability reignites the question of how IL-1 can be released from these cells. IL-1 family cytokines have a diameter of 4.5 nm (van Oostrum et al., 1991), which is theoretically narrow enough to pass through the GSDMD pore (inner diameter of 10–15 nm) (Liu et al., 2016; Sborgi et al., 2016).

Herein, we report that GSDMD is required for IL-1 release under conditions of macrophage hyperactivation and under pyroptosis-inducing conditions where plasma membrane rupture is experimentally prevented. Using reconstituted 293T cells and liposome-based analyses, we provide evidence that GSDMD pores serve as conduits for the transport of IL-1 family cytokines across intact lipid bilayers.

RESULTS

GSDMD Regulates Inflammasome-Induced Pore Formation and IL-1 Release from Intact Cells

Pyroptotic cells are commonly defined as necrotic cells whose plasma membranes have been ruptured by inflammasome-dependent events. This loss of membrane integrity results in the release of cytosolic lactate dehydrogenase (LDH) into the extracellular space, and the staining of intracellular nucleic acids by the membrane impermeable dye propidium iodide (PI) (Davis et al., 2011; Latz et al., 2013). As PI can pass through pores that form in intact cells (Fink and Cookson, 2006), PI staining alone cannot unequivocally identify lysed cells. We consider pyroptotic events those that result in LDH release and PI staining.

To determine whether GSDMD influences IL-1 release from intact cells, we utilized the osmoprotectant glycine to prevent pyroptosis-associated membrane rupture (Fink and Cookson, 2006). Glycine was used to prevent membrane rupture downstream of the normally pyroptotic NLRP3 inflammasome activator nigericin after LPS priming (Latz et al., 2013). Using immortalized bone-marrow-derived macrophages (iBMDMs), LPS treatment alone (or nigericin alone) did not induce LDH release into the extracellular media (Figure 1A). In contrast, LDH release was observed when LPS-primed cells were exposed to nigericin (Figure 1A). Accompanying LDH release was the release of IL-1β (Figure 1B), and the cell population exhibited signs of pore formation, as assessed by real time monitoring of PI staining (Figure 1C). Glycine buffering of the extracellular media almost completely prevented LDH release (Figure 1A), but pore formation and IL-1β release were largely unaffected (Figures 1B and 1C). These findings support the idea that PI staining identifies intact cells that contain pores and cells whose plasma membranes have ruptured. LDH release, in contrast, is specifically indicative of pyroptosis.

To determine whether GSDMD regulates nigericin-induced pore formation and IL-1β release, we used Cas9-based reverse genetics to inactivate *Gsdmd* in iBMDM. Specifically, we used two gRNAs to generate *Gsdmd*$^{-/-}$ iBMDMs. These gRNAs were validated for *Gsdmd* ablation in iBMDMs or mice (Shi et al., 2015). This approach resulted in the elimination of the GSDMD protein from two independent clonal iBMDM populations (Figure S1A). *Gsdmd*$^{-/-}$ cells displayed all expected phenotypes (Shi et al., 2015), in that they could not release LDH, could not form pores, and could not release IL-1β upon LPS and nigericin treatment (Figures 1A–1C, and S1B–S1D). LPS-induced tumor necrosis alpha (TNF-α) secretion was largely unaffected by GSDMD deficiency (Figure S1E). *Gsdmd*$^{-/-}$ cells also retained the ability to form active inflammasomes after LPS priming with subsequent nigericin treatment, as evidenced by the presence of cleaved IL-1β in *Gsdmd*$^{-/-}$ lysates (Figure 1D). The ability of nigericin to induce LDH release IL-1β release, and pore formation was sensitive to high concentrations of extracellular potassium (Figures S1F–S1H), as expected (Perregaux and Gabel, 1994). These observations are consistent with the role of GSDMD as a pyroptosis effector that acts downstream of inflammasome assembly.

In the presence or absence of glycine, *Gsdmd*$^{-/-}$ cells were unable to form pores or release IL-1β (Figures 1B and 1C). Immunoblot analysis verified these results, because the cleaved fragment of IL-1β was present in the extracellular media of nigericin-treated wild-type (WT) cells that were primed with LPS, in the presence or absence of glycine (Figure 1E). In contrast, *Gsdmd*$^{-/-}$ cells were unable to release cleaved IL-1β (Figure 1E), even though this cleaved fragment was detected in cell lysates (Figure 1D). These data indicate that IL-1β can be released from intact cells and that GSDMD is required for this process.

To complement this analysis, we utilized Flatox as an activator of the NAIP-NLRC4 inflammasome. Flatox is an anthrax toxin derivative that consists of a lethal factor-flagellin fusion protein (LFn-Fla) and protective antigen (PA) (von Moltke et al., 2012). When PA and LFn-Fla are combined, Flatox is formed, which delivers flagellin into the cytosol where it activates pyroptosis (von Moltke et al., 2012). Flatox-treated cells induced LDH release from iBMDM (Figure 1F), but IL-1β release was only observed if cells were primed with LPS (Figure 1G). LFn-Fla treatments in the absence of PA led to no LDH release (Figure 1F). Glycine buffering of the extracellular media almost completely prevented LDH release induced by Flatox (Figure 1F), but did not prevent pore formation or IL-1β release (Figures 1G and 1H). Under all conditions examined, *Gsdmd*$^{-/-}$ cells were unable to form pores, release IL-1β or LDH (Figure 1F–1H). Immunoblot analysis demonstrated that GSDMD was not required for IL-1β processing in the cytosol (Figure 1I), but no cleaved IL-1β was detected in the extracellular media of *Gsdmd*$^{-/-}$ cells (Figure 1J). GSDMD was not required for LPS-induced TNF-α secretion (Figure S1I). These data indicate that GSDMD is required for pore formation and IL-1β release in response to activators of distinct inflammasomes, even when lysis is prevented.

GSDMD Is Required for IL-1 Release from Hyperactive Macrophages That Were Stimulated by Bacteria and Their Products

Naturally, pyroptosis and IL-1β release can be uncoupled under conditions of cell hyperactivation, where phagocytes release IL-1β while maintaining viability. To determine whether GSDMD regulates IL-1β release from living cells, we utilized *S. aureus* mutants that lack the gene encoding O-acetyltransferase A (OatA). This strain induces NLRP3-dependent IL-1β release from living macrophages (Shimada et al., 2010; Wolf et al., 2016). Consistent with this idea, we found that OatA-deficient *S. aureus* did not induce LDH release from iBMDMs (Figure 2A), but did promote pore formation and IL-1β release (Figures 2B and 2C). The extent of pore formation observed during bacterial infection was less than that observed for pyroptotic stimuli (compare PI staining in Figure 2C to similar experiments in Figure 1). This difference in the extent of pore formation might explain the ability of these infected macrophages to achieve a state of hyperactivation, as opposed to pyroptosis.

In contrast to WT cells, OatA-deficient *S. aureus* could not induce pore formation or IL-1β or IL-1α release in *Gsdmd*$^{-/-}$ cells (Figures 2B–2D). A second clonal population of *Gsdmd*$^{-/-}$ macrophages yielded similar results (Figures S2A and S2B). Immunoblot analysis demonstrated that GSDMD was necessary for the release of cleaved IL-1β during infection but was not necessary for IL-1β processing within cells (Figures 2E and 2F).

To determine whether PGN or NAG induce GSDMD-dependent IL-1β release, we treated cells with PGN or transfected NAG into the cytosol. PGN treatment or NAG transfection did

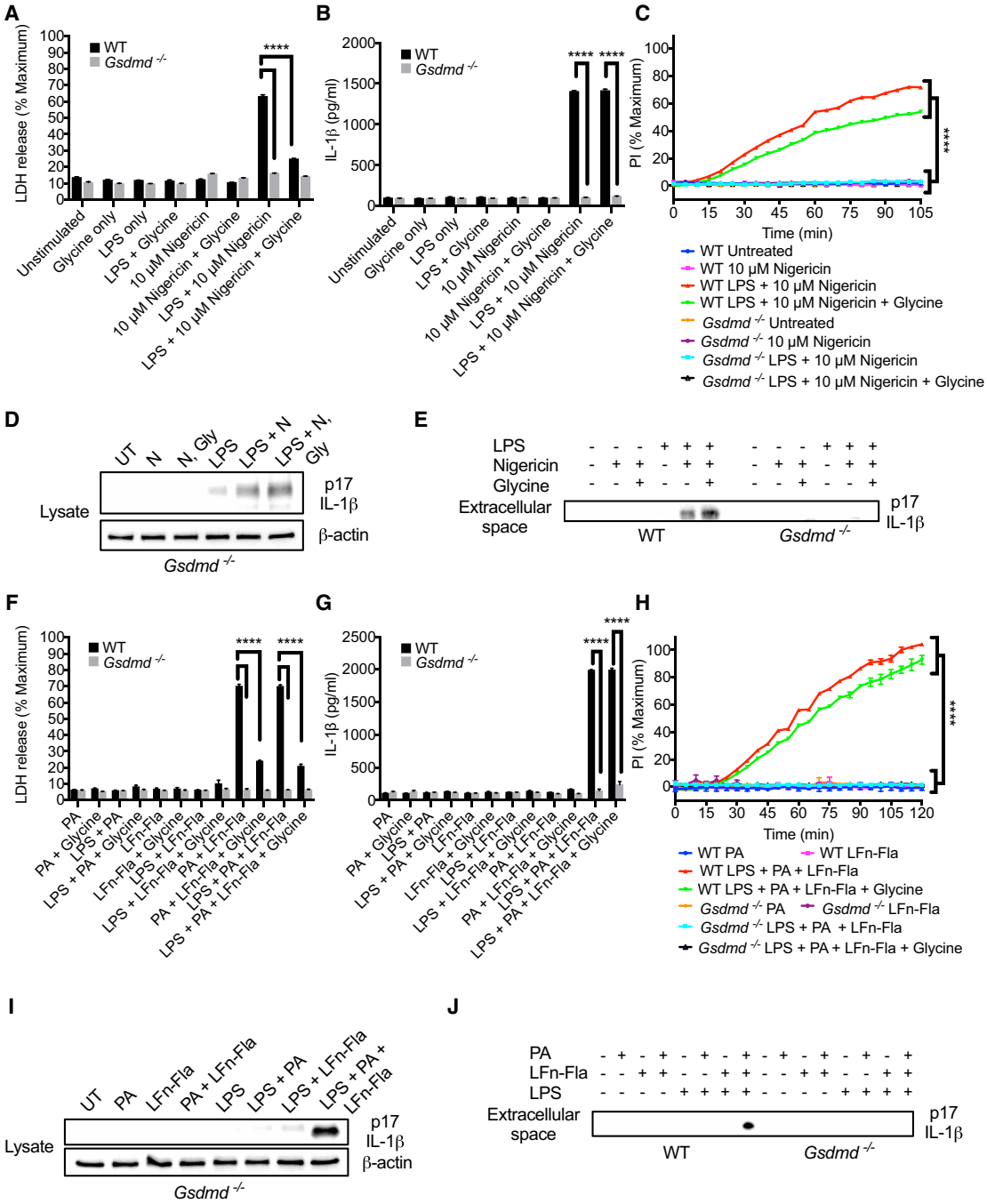

Figure 1. GSDMD Is Required for IL-1β Release when Lysis Is Prevented

(A and F) WT and *Gsdmd*$^{-/-}$ iBMDMs were primed with LPS for 3 hr (or were not primed), and then treated with nigericin for 2 hr (A) or Flatox (PA+LFn-Fla) for 2 hr (F). Stimulations contained 0 mM Glycine or 5 mM Glycine. LDH present in the extracellular media was then quantified.

(B and G) WT and *Gsdmd*$^{-/-}$ iBMDMs were primed with LPS for 3 hr (or not), and then treated with nigericin for 2 hr or Flatox (2 μg/ml PA and 0.5 μg/ml LFn-Fla) for 2 hr. Stimulations contained 0 mM Glycine or 5 mM Glycine. IL-1β release was monitored by ELISA.

(C and H) WT and *Gsdmd*$^{-/-}$ iBMDMs were primed with LPS for 3 hr (or not), and then treated with nigericin for 2 hr or Flatox (PA+LFn-Fla) for 2 hr. Stimulations contained 0 mM Glycine or 5 mM Glycine. PI (5 μM) was added to assay membrane permeability over time.

(D and E) Immunoblot analysis of cell-associated (D) or extracellular (E) IL-1β in *Gsdmd*$^{-/-}$ iBMDMs after 3 hr of LPS priming (or not) and 30 min of nigericin (N) treatment. Stimulations contained 0 mM Glycine (Gly) or 5 mM Glycine.

(I and J) Immunoblot analysis of cell-associated cleaved (I) or extracellular (J) IL-1β in *Gsdmd*$^{-/-}$ iBMDMs after 3 hr of LPS priming (or not) and 2 hr of Flatox treatment at 2 μg/ml PA and 0.5 μg/ml LFn-Fla. Data with error bars are represented as mean ± SEM. Each panel is a representative experiment of at least 3 repeats. ****$p < 0.0001$ as determined by two-way ANOVA with Tukey's multicomparison correction. UT (Untreated cells).

See also Figure S1.

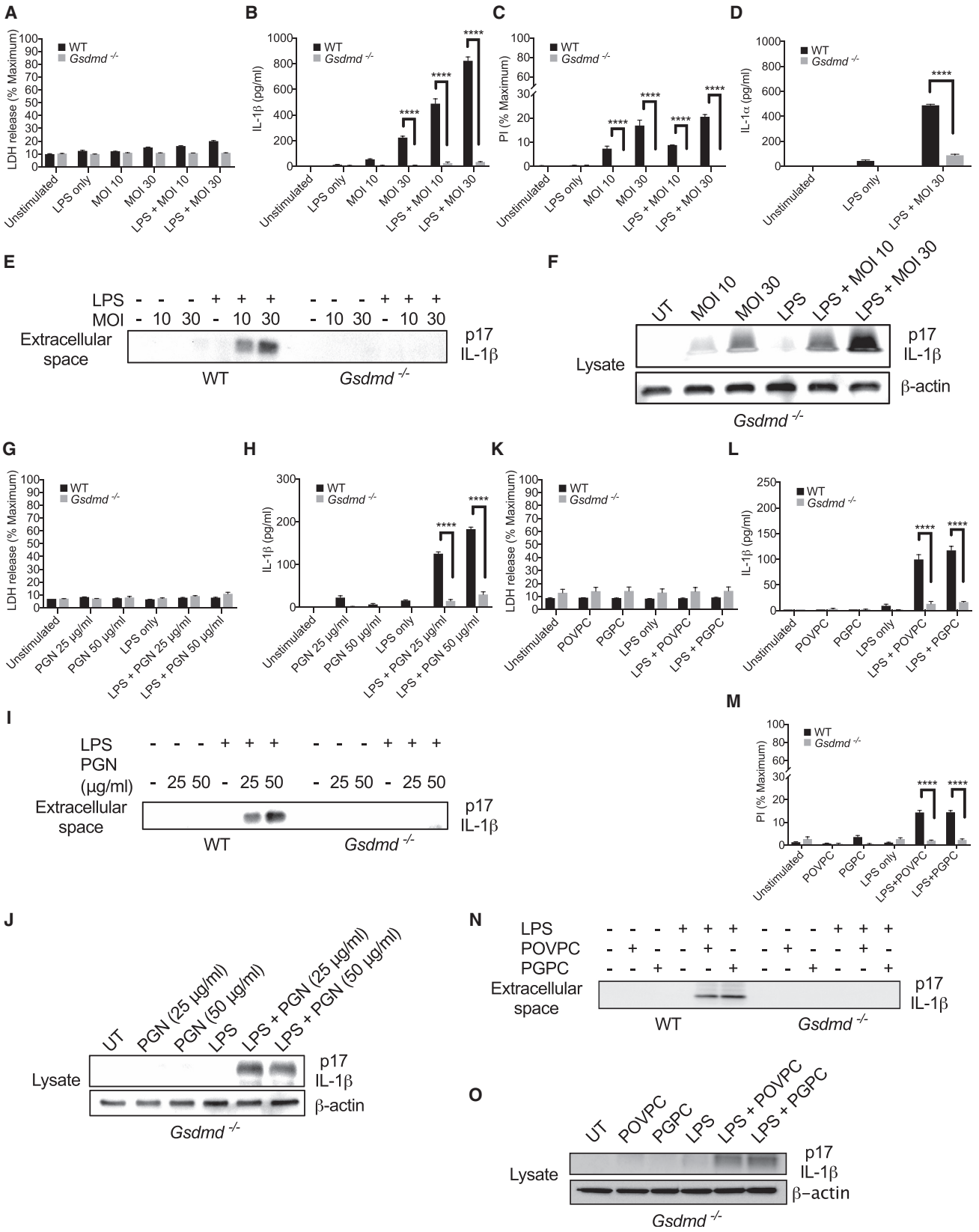

(legend on next page)

not induce LDH release (Figure 2G, S2C), but did induce IL-1β release (Figure 2H, S2D). Under these conditions, *Gsdmd*$^{-/-}$ cells released no IL-1β (Figure 2H, S2D). Although *Gsdmd*$^{-/-}$ cells did not release cleaved IL-1β (Figure 2I, S2E), lysates from *Gsdmd*$^{-/-}$ cells contained cleaved IL-1β (Figure 2J, S2F). Thus, the ability of several microbial hyperactivating stimuli to induce IL-1 release is dependent on GSDMD.

GSDMD Controls IL-1 Release from Macrophages Stimulated with oxPAPC Components

In addition to microbial products, self-derived damage-associated molecular patterns (DAMPs) induce macrophage hyperactivation. For example, isolated lipid components from oxPAPC induce NLRP3-dependent IL-1 release from living macrophages (Zanoni et al., 2017). These lipids are PGPC (1-palmitoyl-2-glutaryl-*sn*-glycero-3-phosphocholine) and POVPC (1-palmitoyl-2-(5′-oxo-valeroyl)-*sn*-glycero-3-phosphocholine). We treated LPS-primed macrophages with PGPC or POVPC and observed pore formation and IL-1β release, but no release of LDH (Figures 2K–2M). No IL-1β was released from *Gsdmd*$^{-/-}$ cells, and these cells were also defective for pore formation in response to PGPC or POVPC (Figures 2L and 2M). A second clonal population of *Gsdmd*$^{-/-}$ cells yielded similar results (Figures S2G and S2H). In addition, no cleaved IL-1β was detected in the extracellular media of *Gsdmd*$^{-/-}$ cells (Figure 2N), whereas cleaved IL-1β was detected in the *Gsdmd*$^{-/-}$ lysates (Figure 2O). oxPAPC component lipids were similar to *S. aureus* in their ability to elicit IL-1β release by a process that is largely insensitive to high concentrations of extracellular potassium (Figures S2I–S2L). oxPAPC components and *S. aureus* therefore induce a mechanism of NLRP3 activation that is distinct from that induced by traditional pyroptotic stimulators of NLRP3, in that high extracellular potassium prevents the activity of the latter (Figures S1F–S1H). These data indicate that several DAMPs that hyperactivate macrophages promote the GSDMD-dependent release of IL-1.

Multiple Stimuli That Hyperactivate Macrophages Promote Inflammasome Assembly within Living Cells

If hyperactive phagocytes truly represent viable cells that release IL-1, then we should be able to visualize inflammasomes within living cells. To test this hypothesis, we used primary macrophages from mice containing a transgene for the inflammasome adaptor ASC, which was fused to the fluorescent protein citrine (Tzeng et al., 2016). The ASC-citrine protein allowed us to identify cells that contained ASC "specks"—which are recognized as inflammasomes (Stutz et al., 2013). LPS-primed primary macrophages from these mice released IL-1β upon treatment with nigericin, ATP, PGN, OatA-deficient *S. aureus*, PGPC, or POVPC (Figures S3A–S3D). LPS-primed cells stimulated with nigericin and ATP appeared swollen and rounded (Figure S3E), which are characteristic features of pyroptosis (Fink and Cookson, 2006). LPS treatment alone or treatment of LPS-primed macrophages with OatA-deficient *S. aureus*, PGN, PGPC, or POVPC did not induce cell rounding or swelling, and the cells remained adherent to the plate (Figure S3E). Thus, macrophages derived from ASC-citrine expressing mice behaved similarly to other macrophages used in this study and elsewhere (Wolf et al., 2016; Zanoni et al., 2016).

Cells were stimulated with LPS alone or were primed with LPS and treated with pyroptotic or hyperactivating stimuli. 16–22 hr later, live cell confocal microscopy was used to identify macrophages containing ASC specks. ASC speck-containing cells

Figure 2. GSDMD Regulates IL-1β Release in Response to Bacteria and Oxidized Lipids that Hyperactivate Macrophages

(A) WT and *Gsdmd*$^{-/-}$ iBMDMs were primed with LPS for 4 hr (or not), and then infected with SA113 Δ*oatA* bacteria at an MOI of 10 and 30 for 12 hr. LDH present in the extracellular media was then quantified.

(B) WT and *Gsdmd*$^{-/-}$ iBMDMs were primed with LPS for 4 hr (or not), and then infected with SA113 Δ*oatA* bacteria at an MOI of 10 and 30 for 12 hr. IL-1β release was monitored by ELISA.

(C) WT and *Gsdmd*$^{-/-}$ iBMDMs were primed with LPS for 4 hr (or not), and then infected with SA113 Δ*oatA* bacteria at an MOI of 10 and 30 for 12 hr with PI (5 μM) in the culture media during infection. Pore formation was assessed after 12 hr by quantifying PI fluorescence intensity.

(D) WT and *Gsdmd*$^{-/-}$ iBMDMs were primed with LPS for 4 hr (or not), and then infected with SA113 Δ*oatA* for 12 hr at an MOI 30 for 12 hr. IL-1β release was monitored by ELISA.

(E) Immunoblot analysis of cleaved IL-1β in the extracellular media of WT and *Gsdmd*$^{-/-}$ iBMDMs after 4 hr of LPS priming (or not), and then infected with SA113 Δ*oatA* for 12 hr at an MOI of 10 and 30.

(F) Immunoblot analysis of cleaved IL-1β in lysates of WT and *Gsdmd*$^{-/-}$ iBMDMs after 4 hr of LPS priming (or not), and then infected with SA113 Δ*oatA* for 12 hr at an MOI of 10 and 30.

(G) WT and *Gsdmd*$^{-/-}$ iBMDMs were primed with LPS for 4 hr (or not), and then treated with PGN for 6 hr. LDH present in the extracellular media was then quantified.

(H) WT and *Gsdmd*$^{-/-}$ iBMDMs were primed with LPS for 4 hr (or not), and then treated with PGN for 6 hr. IL-1β release was monitored by ELISA.

(I) Immunoblot analysis of cleaved IL-1β in the extracellular media of WT and *Gsdmd*$^{-/-}$ iBMDMs after 4 hr of LPS priming (or not), and then treated with PGN for 6 hr.

(J) Immunoblot analysis of cleaved IL-1β in lysates of *Gsdmd*$^{-/-}$ iBMDMs after 4 hr of LPS priming (or not), and then treated with PGN for 6 hr.

(K) WT and *Gsdmd*$^{-/-}$ iBMDMs were primed with LPS for 4 hr (or not), and then treated with PGPC or POVPC for 6 hr. LDH present in the extracellular media was then quantified.

(L) WT and *Gsdmd*$^{-/-}$ iBMDMs were primed with LPS for 4 hr (or not), and then treated with PGPC or POVPC for 6 hr. IL-1β release was monitored by ELISA.

(M) WT and *Gsdmd*$^{-/-}$ iBMDMs were primed with LPS for 4 hr (or not), and then treated with PGPC or POVPC for 6 hr with PI (5 μM) in the culture media. Pore formation was assessed after 6 hr by quantifying PI fluorescence intensity.

(N) Immunoblot analysis of cleaved IL-1β of cell culture supernatants from WT and *Gsdmd*$^{-/-}$ iBMDMs after 4 hr of LPS priming (or not), and then challenged with PGPC or POVPC for 6 hr.

(O) Immunoblot analysis of cell-associated cleaved IL-1β in *Gsdmd*$^{-/-}$ iBMDMs after 4 hr of LPS priming (or not), and then challenged with PGPC or POVPC for 6 hr.

Data with error bars are represented as mean ± SEM. Each panel is a representative experiment of at least 3 repeats.

(UT) Untreated cells. See also Figure S2.

were monitored for the ability to maintain mitochondrial membrane potential by staining with MitoTracker Red CMXROS. Alternatively, macrophages were treated with fluorescent zymosan, which allowed us to monitor phagocytic activity. LPS treatment alone did not induce inflammasome assembly, as revealed by a lack of ASC specks in these cells (Figure 3A and Movie S1). These cells exhibited MitoTracker Red CMXROS staining (Figures 3A and 3B) and readily ingested zymosan (Figure 3C, and Movie S1). The opposite finding was made upon inspection of LPS-primed cells that were treated with nigericin or ATP. Under these conditions, ASC specks were formed, yet cells containing specks did not stain for MitoTracker Red CMXROS and were unable to undergo phagocytosis (Figures 3A–3C and Movie S2). The absence of any cellular activities within ATP- or nigericin-treated macrophages supports the idea that these stimuli induce pyroptosis.

LPS-primed cells that were stimulated with PGN, OatA-deficient *S. aureus*, PGPC, or POVPC induced the formation of ASC specks (Figure 3A). The vast majority of ASC speck-containing cells treated with these stimuli retained mitochondrial and phagocytic activity (Figure 3A–3C and Movies S3 and S4). We noted that a small proportion of cells appeared dead after treatment with hyperactive stimuli. Of these stimuli, OatA-deficient *S. aureus* induced the least amount of cell death (Figures 3B and 3C), but induced the highest amount of IL-1β release (Figures S3B–S3D). In contrast, the most toxic hyperactivating stimulus (PGN) (Figures 3B and 3C), induced the lowest amount of IL-1β release (Figures S3B–S3D). This anti-correlation between cell death and IL-1β release that is associated with hyperactivating stimuli supports the idea that these inflammasome activators induce IL-1 release from living cells that contain ASC specks.

IL-1β Release Occurs Upon GSDMD Pore Formation in the Plasma Membrane of Intact Cells

To determine whether GSDMD pores facilitate the secretion of proteins from living cells, we used 293T cells as a model. We created cDNAs encoding the N- and C-terminal fragments of GSDMD (NT-GSDMD-EGFP and CT-GSDMD-EGFP), and full-length GSDMD (GSDMD-EGFP), each containing an EGFP tag. Plasmids encoding each of these GSDMD alleles were electroporated into 293T cells that were stably producing a fluorescent IL-1β-tdTomato fusion protein. Rupture of the plasma membrane during our analysis was prevented by performing all experiments in the presence of glycine.

Forward and side scatter analysis by flow cytometry focused attention on intact cells (Figure S4A). At 6 hr post electroporation, all *Gsdmd* alleles were expressed detectably, except the GSDMD N terminus (Figure 4A). Thus, we included in our analysis a hypomorphic GSDMD N terminus that contains an I105N mutation (Kayagaki et al., 2015). This mutation reduces the efficiency of pore formation and renders this protein more detectable within cells than the WT GSDMD N terminus (Aglietti et al., 2016) (Figure 4A).

To determine which GSDMD variant induced pore formation, we stained cells with the membrane impermeable DNA dye 7-AAD. Two functionally distinct groups of GSDMD variants were identified. One group exhibited low intensity 7-AAD staining and consisted of full-length GSDMD, its C-terminal fragment, and full-length GSDMD I105N (Figures 4B, S4B). The second group exhibited high intensity 7-AAD staining and consisted of the N-terminal pore-forming fragments of WT and I105N GSDMD (Figures 4B, S4B). To determine whether pore-forming activity correlated with IL-1β release, IL-1β-tdTomato fluorescence intensity was monitored. We observed a transition from a single tdTomato positive population at 0 hr to positive and negative populations at 7 hr post electroporation (Figures 4C and 4D). The pore forming N-terminal WT and I105N GSDMD fragments exhibited similar and substantial decrease in red fluorescence over time (Figures 4C and 4D). In contrast, the full-length GSDMD, its C-terminal fragment, and full-length GSDMD I105N exhibited minimal loss of red fluorescence over time (Figures 4C and 4D). The pore-forming activity of GSDMD therefore correlates with the ability of cells to release IL-1β. These studies suggest that the GSDMD pore is sufficient to mediate IL-1 release from intact cells.

IL-1 Family Cytokines Pass through GSDMD Pores That Form in Intact Liposomes

The correlation between pore formation and IL-1β release in intact cells suggests that GSDMD pores serve as a conduit for IL-1β secretion. To test this possibility, a reductionist approach was taken to examine the release of IL-1β from the lumen of liposomes. We generated liposomes that consist of 1-palmitoyl-2-oleoyl-sn-glycero-3-phosphocholine (PC) and 1,2-dioleoyl-sn-glycero-3-(phospho-l-serine) (PS). Electron microscopy of liposomes treated with GSDMD or caspase-11 did not reveal evidence of pore formation (Figures 4E and 4F). In contrast, GSDMD and caspase-11 co-treatment generated liposomes that contained pores (Figure 4G), as expected (Aglietti et al., 2016; Ding et al., 2016; Liu et al., 2016; Sborgi et al., 2016). To determine whether GSDMD pores stimulated membrane rupture, liposomes were generated in the presence of fluorescent dextrans of variable sizes. No dextran release was observed when liposomes were treated with caspase-11, but dextran release was observed upon GSDMD and caspase-11 co-treatment (Figure S4C). Dextrans with a diameter smaller than the GSDMD pore passed into the extra-liposomal space (4 kDa and 20 kDa with hydrodynamic radii of less than 4 nm) (Armstrong et al., 2004) (Figure S4C). By contrast, dextrans with hydrodynamic radii of 27 nm (2,000 kDa) were largely retained in the liposome lumen (Figure S4C). We also examined the release of enzymatically active tetrameric LDH from the liposome lumen, which has a diameter of 10 nm (Kovacs and Miao, 2017). LDH release was minimal under conditions of GSDMD and caspase-11 co-treatment (Figure S4D). These data indicate that GSDMD generates pores within intact liposomes.

Similar studies were performed to determine whether GSDMD pores facilitate IL-1β release from the liposome lumen. Treatment with GSDMD or caspase-11 did not release IL-1β (Figures 4H and 4I). In contrast, treatment of liposomes with GSDMD and caspase-11 induced the release of ~80% of the total IL-1β that was present in the lumen (Figures 4H and 4I). Similar results were obtained when we examined IL-18 release (Figures 4J and 4K). These findings are similar to what we observe under conditions of cell hyperactivation, where IL-1 family cytokines, but not LDH, are released from intact cells. These collective results raise the possibility that GSDMD, in addition to promoting pyroptosis, serves as a direct conduit for the release of IL-1 family cytokines.

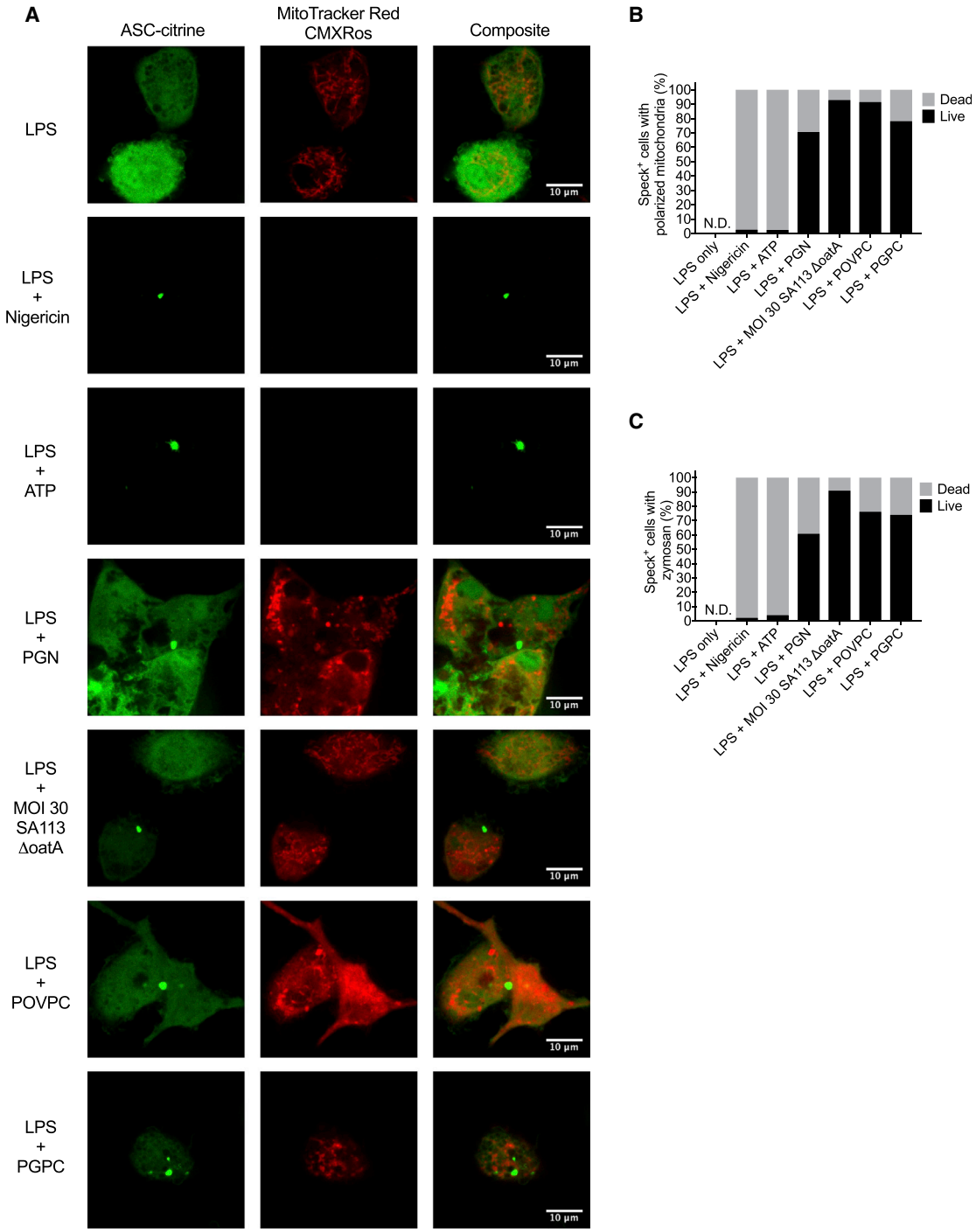

Figure 3. Hyperactive Stimuli Induce Inflammasome Assembly within Living Macrophages

(A) Confocal imaging in the red and green channels of live cell ASC-citrine expressing BMDMs primed with LPS for 3 hr, with second stimulations of nigericin, 5 mM ATP, 50 μg/ml PGN, MOI 30 of SA113 Δ*oatA*, POVPC, or PGPC for 16–22 hr. Red signal corresponds to MitoTracker Red CMXRos. Green signal corresponds to ASC-citrine fusion protein diffusely cytosolic or oligomerized into inflammasome specks.

(B) Enumeration of cells with visible ASC specks that also contain polarized mitochondria as a sign of viability. ($n \geq 25$ speck containing cells per condition)

(C) Enumeration of cells with visible ASC specks that also phagocytose zymosan particles as a sign of viability. ($n \geq 8$ speck containing cells per condition)

See also Figure S3.

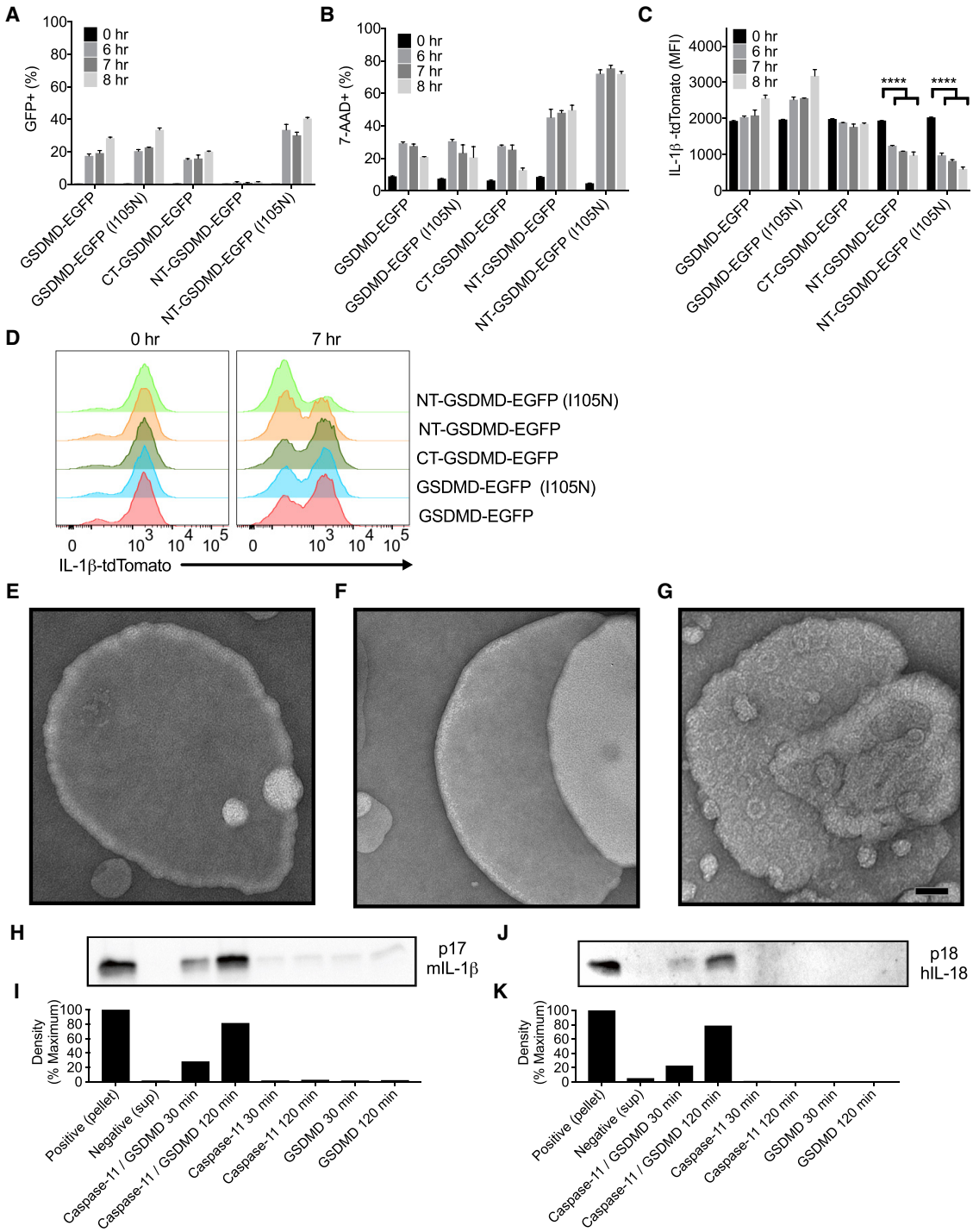

Figure 4. Cleaved GSDMD Acts as a Conduit for the Release of Cytosolic or Encapsulated IL-1 Family Members

(A) EGFP signal was monitored by flow cytometry in 293T cells stably expressing IL-1β-tdTomato after electroporation with GSDMD alleles tagged with EGFP.

(B) 7-AAD signal was monitored by flow cytometry in 293T cells stably expressing IL-1β-tdTomato after electroporation with GSDMD alleles tagged with EGFP.

(C) tdTomato signal was monitored by flow cytometry in 293T cells stably expressing IL-1β-tdTomato after electroporation with GSDMD alleles tagged with EGFP.

(D) Representative histogram of tdTomato fluorescence overlays for 0 and 7 hr post electroporation with GSDMD alleles tagged with EGFP.

(E–G) EM micrographs of PC:PS unextruded liposomes treated with recombinant GSDMD alone (E) caspase-11 alone (F) or with combined treatment (G). Scale bar equals 50 nm.

(H) Immunoblot analysis of IL-1β present within liposomes (pellet), or supernatants after ultracentrifugation of liposomes that were untreated, treated with caspase-11, or treated with caspase-11 and GSDMD for 30 and 120 min.

(legend continued on next page)

DISCUSSION

Based on data presented in this study, we propose that GSDMD has distinct functions in the context of two different cell-fate decisions. One function is to execute the process of cell death, which occurs when the cell-fate decision of pyroptosis is made. This activity of GSDMD results in the indirect release of IL-1 after membrane disruption. The pyroptotic cell-fate decision offers the benefit of a massive inflammatory response that can be induced locally, at the site of infection. However, the cost of pyroptosis is that the dead cell can no longer participate in any immunomodulatory activities. These costs and benefits are somewhat balanced by the second cell-fate decision that we now consider to be mediated by GSDMD—cell hyperactivation. The benefit of this cell-fate decision is that the phagocyte can add IL-1 family cytokines to the repertoire of secreted factors and that these cells might continue to influence immunomodulatory events. Indeed, conditions inducing dendritic cell hyperactivation lead to stronger antigen-specific T cell responses in mice than those that induce traditional dendritic cell activation states (Zanoni et al., 2016). The cost of cell hyperactivation, however, might be that a more modest abundance of IL-1 in the infected tissue is achieved, as compared to a pyroptotic cell-fate decision.

Central to our working hypothesis is that hyperactive cells are alive. In this study, we provided additional data to support this claim, as live cell microscopy revealed hyperactive cells containing inflammasomes, and most of these cells maintained mitochondrial and phagocytic activity. This ability to maintain biological activities after inflammasome assembly is a hallmark of cell viability and supports our conclusion that hyperactivating stimuli induce IL-1 release from living cells.

The presence of a small percent of dead cells that have been exposed to hyperactivating stimuli is worth discussing. These dead cells likely contribute to some of the IL-1 release observed under hyperactivating conditions because these cells contain inflammasomes. However, three lines of evidence invalidate the suggestion that these dead cells are the sole source of IL-1 released into the extracellular media. First, a comparison of several hyperactivating stimuli revealed an anti-correlation between amount of IL-1β release and the extent of cell death. If dead cells were solely responsible for IL-1 release, then a direct correlation should be observed. Second, NLRP3 stimuli that promoted pyroptosis were sensitive to high extracellular potassium concentrations, whereas NLRP3 stimuli that promoted cell hyperactivation were largely insensitive to similar treatments. This finding is inconsistent with the idea that hyperactivating stimuli are merely weak activators of pyroptosis. Third, if we were to propose that dead cells were the sole source of extracellular IL-1, then we must also propose that the vast majority of living hyperactive cells that contain inflammasomes are unable to process IL-1 and GSDMD. Based on the compendium of evidence supporting inflammasomes as the sites of IL-1 and GSDMD processing, this possibility is unlikely. We do, however, recognize the limitations of our assays, in that we have demonstrated a genetic requirement of GSDMD for IL-1 release from macrophages, but have used model 293T cells and liposomes to monitor protein secretion. Unimpeachable evidence supporting our conclusions awaits the development of assays that monitor viability, inflammasome assembly, and IL-1 release simultaneously from single cells. Despite this caveat, the simplest interpretation of our data is that GSDMD pores represent a mechanism of IL-1 secretion from hyperactive cells. Validation of this hypothesis would provide a mandate to better understand the conventional and unconventional mechanisms of cytokine release in the innate immune system.

STAR★METHODS

Detailed methods are provided in the online version of this paper and include the following:

- KEY RESOURCES TABLE
- CONTACT FOR REAGENT AND RESOURCE SHARING
- EXPERIMENTAL MODEL AND SUBJECT DETAILS
  - Cell lines, Transfection, and Retroviral Transduction
  - Generation of *Gsdmd*-Deficient iBMDMs
  - Differentiation of ASC-Citrine Bone Marrow Derived Macrophages
  - Immortalization Protocol for Bone Marrow Derived Macrophages
- METHOD DETAILS
  - Ligand and Chemical Reconstitution
  - LDH Assay, ELISAs, and Antibody Usage
  - Real-Time Cell Permeability Plate Reader Assay
  - Bacterial Infections with SA113 Δ*oatA*
  - Live-Cell Imaging of Cells with Inflammasome Specks
  - Neon Electroporation
  - Flow Cytometric Analysis of Electroporated Cells
  - Protein Expression and Purification
  - Liposome Encapsulation, Pore-Dependent Release Assay, and Electron Microscopy
- QUANTIFICATION AND STATISTICAL ANALYSIS

SUPPLEMENTAL INFORMATION

Supplemental Information includes four figures and four movies and can be found with this article online at https://doi.org/10.1016/j.immuni.2017.11.013.

AUTHOR CONTRIBUTIONS

C.L.E. and Y.T. designed and performed experiments. J.R., S.X., and H.W. provided reagents and performed electron microscopy. J.C.K. supervised all research. All authors discussed results and commented on the manuscript.

(I) Densitometry quantification of western blot band density for IL-1β release from liposomes.
(J) Immunoblot analysis of IL-18 present within liposomes (pellet), or supernatants after ultracentrifugation of liposomes that were untreated, treated with caspase-11, or treated with caspase-11 and GSDMD for 30 and 120 min.
(K) Densitometry quantification of western band density for IL-18 release from liposomes.
Data with error bars are represented as mean ± SEM. Each panel is a representative experiment of at least 3 repeats.
See also Figure S4.

ACKNOWLEDGMENTS

We thank Douglas Golenbock, Russell Vance, and David Underhill for providing essential reagents. This work was supported by NIH grants AI093589 and AI116550 to J.C.K., and NIH grants HD087988 and AI124491 to H.W. J.C.K. holds an Investigators in the Pathogenesis of Infectious Disease Award from the Burroughs Wellcome Fund. C.L.E. is supported by the Harvard Herchel Smith and Landry Cancer Biology Fellowships. Y.T. is a postdoctoral fellow of the Jane Coffin Childs Fund (the Merck Fellow).

Received: June 23, 2017
Revised: September 12, 2017
Accepted: November 10, 2017
Published: November 28, 2017

REFERENCES

Aglietti, R.A., Estevez, A., Gupta, A., Ramirez, M.G., Liu, P.S., Kayagaki, N., Ciferri, C., Dixit, V.M., and Dueber, E.C. (2016). GsdmD p30 elicited by caspase-11 during pyroptosis forms pores in membranes. Proc. Natl. Acad. Sci. USA *113*, 7858–7863.

Armstrong, J.K., Wenby, R.B., Meiselman, H.J., and Fisher, T.C. (2004). The hydrodynamic radii of macromolecules and their effect on red blood cell aggregation. Biophys. J. *87*, 4259–4270.

Bera, A., Herbert, S., Jakob, A., Vollmer, W., and Götz, F. (2005). Why are pathogenic staphylococci so lysozyme resistant? The peptidoglycan O-acetyltransferase OatA is the major determinant for lysozyme resistance of Staphylococcus aureus. Mol. Microbiol. *55*, 778–787.

Cerretti, D.P., Kozlosky, C.J., Mosley, B., Nelson, N., Van Ness, K., Greenstreet, T.A., March, C.J., Kronheim, S.R., Druck, T., Cannizzaro, L.A., et al. (1992). Molecular cloning of the interleukin-1 beta converting enzyme. Science *256*, 97–100.

Chen, K.W., Groß, C.J., Sotomayor, F.V., Stacey, K.J., Tschopp, J., Sweet, M.J., and Schroder, K. (2014). The neutrophil NLRC4 inflammasome selectively promotes IL-1β maturation without pyroptosis during acute Salmonella challenge. Cell Rep. *8*, 570–582.

Davis, B.K., Wen, H., and Ting, J.P. (2011). The inflammasome NLRs in immunity, inflammation, and associated diseases. Annu. Rev. Immunol. *29*, 707–735.

Ding, J., Wang, K., Liu, W., She, Y., Sun, Q., Shi, J., Sun, H., Wang, D.C., and Shao, F. (2016). Pore-forming activity and structural autoinhibition of the gasdermin family. Nature *535*, 111–116.

Fink, S.L., and Cookson, B.T. (2006). Caspase-1-dependent pore formation during pyroptosis leads to osmotic lysis of infected host macrophages. Cell. Microbiol. *8*, 1812–1825.

Gaidt, M.M., Ebert, T.S., Chauhan, D., Schmidt, T., Schmid-Burgk, J.L., Rapino, F., Robertson, A.A., Cooper, M.A., Graf, T., and Hornung, V. (2016). Human Monocytes Engage an Alternative Inflammasome Pathway. Immunity *44*, 833–846.

Garlanda, C., Dinarello, C.A., and Mantovani, A. (2013). The interleukin-1 family: back to the future. Immunity *39*, 1003–1018.

Kagan, J.C., Magupalli, V.G., and Wu, H. (2014). SMOCs: supramolecular organizing centres that control innate immunity. Nat. Rev. Immunol. *14*, 821–826.

Kayagaki, N., Stowe, I.B., Lee, B.L., O'Rourke, K., Anderson, K., Warming, S., Cuellar, T., Haley, B., Roose-Girma, M., Phung, Q.T., et al. (2015). Caspase-11 cleaves gasdermin D for non-canonical inflammasome signalling. Nature *526*, 666–671.

Kovacs, S.B., and Miao, E.A. (2017). Gasdermins: Effectors of Pyroptosis. Trends Cell Biol. *27*, 673–684.

Latz, E., Xiao, T.S., and Stutz, A. (2013). Activation and regulation of the inflammasomes. Nat. Rev. Immunol. *13*, 397–411.

Liu, X., Zhang, Z., Ruan, J., Pan, Y., Magupalli, V.G., Wu, H., and Lieberman, J. (2016). Inflammasome-activated gasdermin D causes pyroptosis by forming membrane pores. Nature *535*, 153–158.

Martinon, F., Burns, K., and Tschopp, J. (2002). The inflammasome: a molecular platform triggering activation of inflammatory caspases and processing of proIL-beta. Mol. Cell *10*, 417–426.

Martinon, F., Mayor, A., and Tschopp, J. (2009). The inflammasomes: guardians of the body. Annu. Rev. Immunol. *27*, 229–265.

Mellman, I., Turley, S.J., and Steinman, R.M. (1998). Antigen processing for amateurs and professionals. Trends Cell Biol. *8*, 231–237.

Perregaux, D., and Gabel, C.A. (1994). Interleukin-1 beta maturation and release in response to ATP and nigericin. Evidence that potassium depletion mediated by these agents is a necessary and common feature of their activity. J. Biol. Chem. *269*, 15195–15203.

Sborgi, L., Rühl, S., Mulvihill, E., Pipercevic, J., Heilig, R., Stahlberg, H., Farady, C.J., Müller, D.J., Broz, P., and Hiller, S. (2016). GSDMD membrane pore formation constitutes the mechanism of pyroptotic cell death. EMBO J. *35*, 1766–1778.

Shi, J., Zhao, Y., Wang, K., Shi, X., Wang, Y., Huang, H., Zhuang, Y., Cai, T., Wang, F., and Shao, F. (2015). Cleavage of GSDMD by inflammatory caspases determines pyroptotic cell death. Nature *526*, 660–665.

Shimada, T., Park, B.G., Wolf, A.J., Brikos, C., Goodridge, H.S., Becker, C.A., Reyes, C.N., Miao, E.A., Aderem, A., Götz, F., et al. (2010). Staphylococcus aureus evades lysozyme-based peptidoglycan digestion that links phagocytosis, inflammasome activation, and IL-1beta secretion. Cell Host Microbe *7*, 38–49.

Stutz, A., Horvath, G.L., Monks, B.G., and Latz, E. (2013). ASC speck formation as a readout for inflammasome activation. Methods Mol. Biol. *1040*, 91–101.

Tzeng, T.C., Schattgen, S., Monks, B., Wang, D., Cerny, A., Latz, E., Fitzgerald, K., and Golenbock, D.T. (2016). A Fluorescent Reporter Mouse for Inflammasome Assembly Demonstrates an Important Role for Cell-Bound and Free ASC Specks during In Vivo Infection. Cell Rep. *16*, 571-82.

van Oostrum, J., Priestle, J.P., Grütter, M.G., and Schmitz, A. (1991). The structure of murine interleukin-1 beta at 2.8 A resolution. J. Struct. Biol. *107*, 189–95.

von Moltke, J., Trinidad, N.J., Moayeri, M., Kintzer, A.F., Wang, S.B., van Rooijen, N., Brown, C.R., Krantz, B.A., Leppla, S.H., Gronert, K., and Vance, R.E. (2012). Rapid induction of inflammatory lipid mediators by the inflammasome in vivo. Nature *490*, 107–111.

Wolf, A.J., Reyes, C.N., Liang, W., Becker, C., Shimada, K., Wheeler, M.L., Cho, H.C., Popescu, N.I., Coggeshall, K.M., Arditi, M., and Underhill, D.M. (2016). Hexokinase Is an Innate Immune Receptor for the Detection of Bacterial Peptidoglycan. Cell *166*, 624–636.

Zanoni, I., Tan, Y., Di Gioia, M., Broggi, A., Ruan, J., Shi, J., Donado, C.A., Shao, F., Wu, H., Springstead, J.R., and Kagan, J.C. (2016). An endogenous caspase-11 ligand elicits interleukin-1 release from living dendritic cells. Science *352*, 1232–1236.

Zanoni, I., Tan, Y., Di Gioia, M., Springstead, J.R., and Kagan, J.C. (2017). By Capturing Inflammatory Lipids Released from Dying Cells, the Receptor CD14 Induces Inflammasome-Dependent Phagocyte Hyperactivation. Immunity *47*, 697–709.e3.

STAR★METHODS

KEY RESOURCES TABLE

REAGENT or RESOURCE	SOURCE	IDENTIFIER
Antibodies		
Rabbit polyclonal Anti-β-Actin	Cell Signaling Technology	#4967; RRID:AB_330288
Mouse monoclonal Anti-β-Actin	Sigma-Aldrich	A5441; RRID:AB_476744
Rabbit polyclonal Anti-IL-1β	Genetex	GTX74034; RRID:AB_378141
Goat polyclonal Anti-IL-1β	R&D Systems	AF-401-NA; RRID:AB_416684
Biotinylated Anti-IL-1β	R&D Systems	BAF401; RRID:AB_416684
Rabbit polyclonal Anti-GSDMDC1	Novus Biologicals	NBP2-33422; RRID:AB_2687913
Rabbit polyclonal Anti-GSDMD (126-138)	Sigma	G7422; RRID:AB_1850381
Mouse monoclonal Anti-IL-18	R&D Systems	D043-3; RRID:AB_356963
Bacterial and Virus Strains		
Staphylococcus aureus: SA113 Δ*OatA*	Bera et al., 2005	N/A
Chemicals, Peptides, and Recombinant Proteins		
E. coli LPS Serotype O111:B4 S-form	Enzo Life Sciences	ALX-581-012-L002
Peptidoglycan from *Staphylococcus aureus*	Sigma	77140-25MG
N-Acetyl-D-glucosamine	Sigma	A8625-25G
POVPC	Cayman Chemical	N° 10031
PGPC	Cayman Chemical	N° 10044
Nigericin	InvivoGen	tlrl-nig-5
Glycine	Sigma	G7126-5KG
KCl	Amresco	0395-1kg
Propidium iodide	Sigma	P4864-10ML
7-AAD	Biolegend	420404
Pierce™ NeutrAvidin™ Agarose	ThermoFisher	29201
18:1 PS (DOPS) in chloroform	Avanti Polar Lipids	840035C
16:0-18:1 PC in chloroform	Avanti Polar Lipids	850457C
FITC-dextran 4 kDa	Sigma	46944-100MG-F
FITC-dextran 20 kDa	Sigma	FD20S-100MG
FITC-dextran 2000 kDa	Sigma	FD2000S-250MG
FluoroBrite™ colorless DMEM	ThermoFisher	A1896701
L-Lactate Dehydrogenase (L-LDH)	Sigma	10127884001
Recombinant Mouse IL-1β (carrier-free)	BioLegend	575104
Recombinant Human IL-18 (carrier-free)	BioLegend	592104
CellMask™ Deep Red Plasma membrane Stain	ThermoFisher	C10046
Zymosan A *S. cerevisiae* BioParticles™, Texas Red™ conjugate	ThermoFisher	Z2843
MitoTracker™ Red CMXRos	ThermoFisher	M7512
OptiMEM	ThermoFisher	31985062
Lipofectamine 2000	ThermoFisher	11668019
Recombinant Protective Antigen (PA)	Russell Vance Laboratory	N/A
Lethal factor Flagellin fusion protein (LFn-Fla)	Russell Vance Laboratory	N/A
Human recombinant gasdermin D (GSDMD)	Hao Wu Laboratory	N/A
Murine recombinant caspase-11	Hao Wu Laboratory	N/A
TSA II™ plates with Sheep Blood	ThermoFisher	B21239X
Todd-Hewitt Broth	Sigma	T1438-500G

(*Continued on next page*)

Continued

REAGENT or RESOURCE	SOURCE	IDENTIFIER
Critical Commercial Assays		
Mouse IL-1β ELISA Kit	ThermoFisher	88-7013-86
Mouse TNFα ELISA Kit	ThermoFisher	88-7324-88
Mouse IL-1α ELISA Kit	ThermoFisher	88-5019-86
Pierce™ LDH Cytotoxicity Assay Kit	ThermoFisher	88954
100 μl Tip Neon Transfection Kit	ThermoFisher	MPK10096
Experimental Models: Cell Lines		
Immortalized bone marrow-derived macrophages	Jonathan Kagan Laboratory	N/A
Lentivirally transduced iBMDMs expressing Cas9	This paper	N/A
Lentivirally transduced iBMDMs expressing Cas9 and guide 1 against GSDMD	This paper	N/A
Lentivirally transduced iBMDMs expressing Cas9 and guide 2 against GSDMD	This paper	N/A
Primary bone marrow-derived macrophages from ASC-citrine Transgenic mouse	Douglas Golenbock Laboratory; Tzeng et al., 2016	N/A
HEK 293T	Jonathan Kagan Laboratory	N/A
Retrovirally transduced HEK 293T expressing IL-1β-tdTomato	This paper	N/A
CREJ2 (cells producing J2 retroviral particles)	Jonathan Kagan Laboratory	N/A
Experimental Models: Organisms/Strains		
Mouse: ASC-citrine transgenic reporter (B6.Cg-Gt(ROSA)$^{26Sortm1.1(CAG-Pycard/mCitrine*,-CD2*)Dtg}$/J)	Douglas Golenbock Laboratory; Tzeng et al., 2016	N/A
Oligonucleotides		
GSDMD guide 1 (5' CAGCATCCTGGCATTCCGAG 3')	Shi et al., 2015	N/A
GSDMD guide 2 (5' AAAGTCTCTGATGTCGTCGA 3')	Shi et al., 2015	N/A
Recombinant DNA		
GSDMD cDNA plasmid	Dharmacon	MMM1013-202765078
pCMV-pro-IL1b	Addgene	Plasmid #73953
pEGFP-N1	Jonathan Kagan Laboratory	N/A
ptdTomato-N1	Addgene	Plasmid #54642
lentiCRISPR v2	Addgene	Plasmid #52961
pGSDMD-EGFP-N1	This paper	N/A
pNT-GSDMD-EGFP-N1	This paper	N/A
pCT-GSDMD-EGFP-N1	This paper	N/A
pGSDMD(I105N)-EGFP-N1	This paper	N/A
pNT-GSDMD(I105N)-EGFP-N1	This paper	N/A
pIL-β-tdTomato-N1	This paper	N/A
psPAX2	Addgene	Plasmid #12260
pCMV-VSV-G	Addgene	Plasmid #8454
pMSCV-IRES-hCD2	Jonathan Kagan Laboratory	N/A
pMSCV-IL-β-tdTomato-IRES-hCD2	This paper	N/A
pCL-Eco	Addgene	Plasmid #12371
Software and Algorithms		
GraphPad Prism 7.0	GraphPad Software	N/A
FlowJo (v10.3.0)	FlowJo	N/A
Microsoft Excel	Microsoft	N/A
SlideBook 6.0	Intelligent Imaging Innovations	N/A
Fiji / ImageJ version 2.0.0	https://imagej.net/Fiji	N/A

(*Continued on next page*)

Continued

REAGENT or RESOURCE	SOURCE	IDENTIFIER
Other		
Live cell imaging, μ-Dish 35 mm, high	Ibidi	81156
Copper support film on grids	Electron Microscopy Sciences	FCF400-Cu
Costar, Black 96 well plate w/ lid, clear flat bottom, TC treated	Costar	3603

CONTACT FOR REAGENT AND RESOURCE SHARING

Further information and requests for resources and reagents should be directed to and will be fulfilled by the Lead Contact, Jonathan C. Kagan (jonathan.kagan@childrens.harvard.edu).

EXPERIMENTAL MODEL AND SUBJECT DETAILS

Cell lines, Transfection, and Retroviral Transduction

Immortalized bone marrow derived macrophages (iBMDMs) were cultured in DMEM containing 10% FBS, Penicillin and Streptomycin (Pen+Strep), and supplements of L-glutamine and sodium pyruvate. This media is referred to below as complete DMEM. Cells were washed in PBS pH 7.4 containing 2 mM EDTA to detach cells for passage. Cells were passaged 1:10 every 3 days. HEK293T cells were cultured in complete DMEM. Cells were washed in PBS pH 7.4 then lifted from culture flasks with 0.25% Trypsin. Trypsin was deactivated by addition of serum containing media. The IL-1β-tdTomato fusion construct was created by PCR amplification of the DNA sequence corresponding to the amino acids of cleaved murine IL-1β with the addition of a starting methionine and terminal BglII and SalI restriction enzyme cut sites. The amplicon and vector ptdTomato-N1 were digested with BglII and SalI enzymes per the manufacturer's instructions. The amplicon and vector were gel extracted and ligated together with T7 ligase. GsdmD-EGFP, NT-GsdmD-EGFP, and CT-GsdmD-EGFP were amplified from mouse GsdmD cDNA and cloned in the same manner into the fusion vector pEGFP-N1. When used to make stably expressing cell lines, fusion constructs were subcloned into the MSCV-IRES-hCD2 retroviral vector by digestion with the restriction enzymes BglII and NotI, gel purified, and ligated with T7 ligase. For generating stable cell lines with transgenes, retrovirus particles were produced by transfecting 293T cells with plasmids pCL-Eco, pCMV-VSV-G, and MSCV-IRES-hCD2 containing the gene of interest. For lentiviral mediated CRISPR/cas9 editing of cells, lentiviral particles were produced by transfecting 293T cells with plasmids psPAX2, pCMV-VSV-G, and lentiCRISPRv2. Plasmids were transfected into HEK293T cells in 10 cm dishes at a confluency of 50%–70% with polyethylenimine (PEI) at a DNA to PEI ratio of 1:3. Media was changed 12 hr post DNA transfection and viral supernatants were collected 24 hr post media change. Viral supernatants were spun at 400 x g to remove cellular debris then passed through a 0.45 μm PVDF filter via syringe. To generate an IL-1β-tdTomato stably transduced cell line, viral supernatants were placed directly on growing 293T cells for 24 hr. These cell lines were sorted based on double positivity of hCD2 surface expression and intrinsic fluorescence from the IL-1β-tdTomato protein.

Generation of *Gsdmd*-Deficient iBMDMs

The *Gsdmd*-targeting lentivirus was packaged using lentiCRISPRv2 system. In brief, iBMDMs were plated into a 6-well tissue culture plate and were transduced the next day with the lentiviral particle expressing Cas9 and one of two *Gsdmd*-specific guide RNAs (CAGCATCCTGGCATTCCGAG, AAAGTCTCTGATGTCGTCGA). At 48 hr-post transduction, fresh media containing 20 μg/ml puromycin was added to select for cells transduced with the *Gsdmd*-targeting lentivirus. The puromycin resistant cells were further subjected to single-cell cloning by limited dilution. After culturing in puromycin-containing media for an additional 2-3 weeks, single colonies were picked, expanded, and then analyzed for GSDMD protein by western analysis. iBMDMs expressing the lentiCRISPRv2 vector with a GFP targeting sequence were used as WT controls.

Differentiation of ASC-Citrine Bone Marrow Derived Macrophages

L929 fibroblast cells producing M-CSF were cultured in complete DMEM. Supernatants from L929 fibroblasts were cleared of cellular debris by spinning at 400 x g for 5 min. Pooled supernatants from several culture flasks were combined and passed through a 0.22 μm filter. M-CSF conditioned supernatants were aliquoted and frozen at −20°C. Leg bones of transgenic ASC-citrine mice were removed from dead mice. Cleaned bones were cut with scissors and flushed with sterile PBS pH 7.4 via syringe. Bone marrow suspension was passed through a 70 μm cell strainer to exclude clumps. Cells were plated at 10E6 bone marrow cells per untreated 10 cm dish in macrophage differentiation media consisting of complete DMEM with 30% L-929 M-CSF conditioned media. Plates were fed with 5 mL of additional macrophage differentiation media on day 3 of differentiation. Cell culture media was removed on day 7 and day 8 cultures. Cells were detached from non-treated plates with cold PBS pH 7.4 containing 2 mM EDTA. Cells were then resuspended in media and plated on 96 well plates for IL-1β release assays and ibidi disposable live cell imaging dishes for imaging studies.

Immortalization Protocol for Bone Marrow Derived Macrophages

Primary BMDMs for immortalization were cultured in complete RPMI with 15% FBS, 30% L929 conditioned supernatant and Pen+Strep. Conditioned supernatant collected from the CREJ2 cell line carrying the J2 retrovirus was used to immortalize primary BMDMs. In brief, differentiated primary BMDMs (day 7) were further incubated with 50% J2 conditioned supernatant and 50% L929 conditioned supernatant for 7 days, with one new batch of mixed J2 supernatant and L929 supernatant added at day 3. Transduced BMDMs were then cultured in complete DMEM plus 30% L929 supernatant until 90% confluent. Cells were then passed into new medium containing 25% L929 supernatant. Following this trend, the L929 supernatant concentration in complete DMEM was decreased by 5% during each passage. The immortalization process was completed when the BMDMs grew normally in complete DMEM in the absence of L929 supernatant.

METHOD DETAILS

Ligand and Chemical Reconstitution

Lipopolysaccharide (LPS) from *E. coli*, serotype 0111:B4 was bought in a ready to use format at a stock concentration of 1 mg/ml from Enzo. LPS was used in assays at a concentration of 1 μg/ml. Nigericin was purchased from Invivogen and suspended in sterile ethanol to a stock concentration of 6.7 mM. Nigericin was used at a concentration of 10 μM. Peptidoglycan (PGN) from *S. aureas* was supplied from Sigma and resuspended in sterile PBS pH 7.4 at a stock concentration of 2 mg/ml. Ligand was vortexed and well mixed prior to dilution and addition to cells as PGN is poorly soluble. N-acetyl glucosamine (NAG) was resuspended at a concentration of 1 M in sterile, freshly opened optiMEM transfection media and complexed with lipofectamine 2000 for transfection into cells. Glycine was purchased from Sigma and prepared as a stock solution of 500 mM in PBS pH 7.4, sterile filtered, and kept at 4°C for no longer than 2 months. KCl was purchased from Amresco and stock solution was prepared in complete DMEM at a concentration of 2M. PA and LFn-Fla protein preparations were kind gifts from Russell Vance (UC Berkeley). Propidium iodide (PI) was purchased from Sigma in a ready to use stock solution at a concentration of 1 mg/ml. 7-AAD was purchased from BioLegend as a ready to use solution and used per manufacture instructions. Recombinant mouse IL-1β and human IL-18 were supplied by BioLegend at a concentration of 0.2 mg/ml in the absence of a carrier protein. L-LDH isolated from rabbit muscle was supplied by Sigma in a ready to use solution at a concentration of 10 mg/ml. Fluorescent FITC conjugated dextrans of various sizes (4 kDa, 20 kDa, and 2000 kDa) were supplied by Sigma and reconstituted in liposome buffer at a concentration of 50 mg/ml. Cell mask deep red plasma membrane dye for live cell imaging was purchased from ThermoFisher in a ready to use format. Red fluorescent zymosan was purchased from ThermoFisher and reconstituted in sterile PBS pH 7.4 through vortex and sonication per the manufacturer's directions. MitoTracker Red CMXRos was purchased from ThermoFisher and used within the range suggested by the manufacturer's protocol. PS and PC lipids were supplied by Avanti polar lipids in chloroform. POVPC and PGPC were supplied by Cayman Chemical. Commercially available POVPC and PGPC were supplied as a solution in ethanol in clear glass vials. To remove the organic solvent, a gentle nitrogen gas stream was used to evaporate the ethanol, leaving only the lipids in the glass vials. Pre-warmed serum-free media was then immediately added to the dried lipids so that the final concentrations of POVPC and PGPC were at 1 mg/ml. Reconstituted lipids were incubated at 37°C for 5 mins and were vortexed vigorously for 10 s before adding to cells. Cells were stimulated with 100 μg/ml of resuspended POVPC or PGPC.

LDH Assay, ELISAs, and Antibody Usage

Cell culture supernatants were cleared of cells by spinning 96 well plates at 400 x g for 5 min. Supernatants were transferred to round bottom, non-treated 96 well plates and spun again at 400 x g for 5 min. Supernatants were once more transferred to a new 96 well plate for use or short-term storage at −20°C. Supernatants were assayed for LDH release freshly after stimulation time courses per the manufacturer's protocol from the Pierce LDH cytotoxicity colorimetric assay kit. Measurements for absorbance readings were performed on a Tecan plate reader at wavelengths of 490 nm and 680 nm. Mouse IL-1β, IL-1α, and TNFα were quantitatively measured from cell-free culture supernatants using the eBioscience Ready-SET-Go! (now ThermoFisher) ELISA kits according to the manufacturer's protocol. Supernatants for immunoprecipitation (IP) were isolated from 6 well cultures. Supernatants were cleared of cells through transfer to 5 mL FACS tubes with tightly sealing caps and spun at 400 x g for 5 min. Supernatants were transferred to a new FACS tubes for IP reaction. IL-1β immunoprecipitation used biotinylated polyclonal goat anti-IL-1β antibody from R&D Systems at 0.5 μg of antibody in conjunction with 20 μL of washed neutravidin agarose beads from ThermoFisher per IP sample. These reactions occurred at 4°C overnight on a wheel rotator. IL-1β from supernatant IPs was blotted with rabbit polyclonal anti-IL-1β antibody from Genetex at a dilution of 1:1000. Cell associated IL-1β in cell lysates was blotted with unconjugated goat anti-IL-1β antibody from R&D Systems at a dilution of 1:500. Cell associated β-actin was assayed for loading control through either mouse monoclonal anti-β-actin from Sigma or rabbit polyclonal anti-β-actin from Cell Signaling at a dilution of 1:5000. Liposome and supernatant associated IL-1β was detected with rabbit polyclonal anti-IL-1β antibody from Genetex at a dilution of 1:1000. Liposome and supernatant associated human IL-18 was detected with mouse monoclonal anti-IL-18 from R&D Systems at a dilution of 1:1000.

Real-Time Cell Permeability Plate Reader Assay

1E5 C9-WT and *Gsdmd*$^{-/-}$ iBMDMs were plated in 200 μL per well of a tissue culture treated, black 96 well plate with flat optical transparent bottoms from Costar. After at least 6 hr, the media was changed with warmed media containing no LPS or 1 μg/ml LPS. After 3 hr of priming with LPS, media was removed and replaced with secondary stimuli in warmed plate reader media

(HBSS + 20 mM HEPES + 10% FBS). Wells had 100 μL 2X PI (10 μM) solution added to them either with no glycine or 2X glycine (10 mM). Lysed positive controls had 100 μL of 2X Triton X (1%) solution made in warmed plate reader media. Untreated wells had 100 μL of warm plate reader media added to them. Nigericin treated cells had 100 μL of 2X Nigericin (20 μM) solution added to their respective wells. PA treated cells had 100 μL of 2X PA (4 μg/ml) added to their respective wells. LFn-Fla treated cells had 100 μL of 2X LFn-Fla (1.0 μg/ml) added to their respective wells. Flatox (PA + LFn-Fla) treated cells has 100 μL of 2X Flatox (4 μg/ml PA + 1.0 μg/ml LFn-Fla) added to their respective wells. Cells were allowed to equilibrate with PI for 10 min in a 37°C incubator. The plate was spun at 400xg for 5 min to ensure all cells were at the bottom of the well prior to adding the plate to the plate reader. A Tecan plate reader was used for real time fluorescence monitoring. The program settings for kinetic PI inclusion assay were bottom reading of fluorescence with an excitation wavelength of 530 nm with a bandwidth of 9 nm and emission wavelength of 617 nm with a bandwidth of 20 nm. Ideal gain was calculated from one of the positive lysed replicate wells to make the signal from that well be 70% of max detectable signal. The number of flashes was set to 25 with an integration time of 20 μs with no lag time or settle time. The machine was set to maintain 37°C for the period of the assay.

Bacterial Infections with SA113 Δ*oatA*

WT and Δ*oatA* SA113 were generous gifts from the lab of David Underhill (Cedars Sinai), and were first identified by Friedrich Götz and colleagues. Glycerol bacterial stocks of SA113 Δ*oatA* were initially streaked to colonies on TSA agar plates containing sheep blood from ThermoFisher. Single colonies were used for individual experiments. Colonies were picked and grown in Todd-Hewitt broth from Sigma supplemented with Kanamycin selection at 50 μg/ml in a volume of 5 mL for 18-24 hr at 37°C while shaking. Cultures were washed 3 times in sterile PBS pH 7.4. Indicated MOI of bacteria were prepared in warm DMEM with 10% FBS, L-glutamine and sodium pyruvate supplementation without antibiotics. Cell culture media was replaced with media of indicated MOI and plates were spun at 400 x g for 5 min to synchronize bacterial uptake by macrophages. Macrophages were either unprimed or primed with 1 μg/ml of LPS for 3-4 hr prior to infection. After 1-2 hr of infection in antibiotic free media, media was replaced with warm DMEM with 10% FBS, L-glutamine and sodium pyruvate supplementation with Pen+Strep antibiotics and supplemented with gentamycin to kill extracellular bacteria. For experiments examining PI staining, PI was included in the culture media to monitor transient pore formation during the 12 hour course of infection. 12 hr post initial infection, LDH was measured on cell-free supernatants from 96 well plates that had been plated with 1E5 macrophages 6 hr prior to priming. Additional supernatants were used for ELISAs. Western analysis of cleaved IL-1β in the supernatant and lysate of macrophages was from 1E6 macrophages plated in 6 well plates 6 hr prior to priming.

Live-Cell Imaging of Cells with Inflammasome Specks

Leg bones from ASC-citrine transgenic mice expressing ubiquitous Cre on a WT ASC background were generous gifts from the lab of Douglas Golenbock (UMASS). ASC-citrine bone marrow cells were differentiated with 30% L929 supernatants containing M-CSF for 7 days in 10 mL of supplemented media on 10 cm untreated suspension cell culture dishes to prevent full adherence. On day 3, 5 mL of supplemented media containing 30% L929 supernatants were added to dishes to feed the cells. On day 7 and 8 cells were used for experiments by gentle lifting with PBS with 2 mM EDTA, cell counting with hemocytometer, and plating 2.5E5 macrophages onto ibidi glass bottom disposable 35 mm, high live cell imaging plates. Plated cells were primed with 1 μg/ml of LPS for 3 hr then stimulated with second stimuli as described elsewhere. Stimuli were left overnight and imaging was conducted the following morning. Bright field images were taken prior to confocal imaging to note general morphology of cells. For mitochondrial potential experiments, MitoTracker Red CMXRos was used at a dilution of 1:7000 and stained for 30 min prior to imaging. Cell mask deep red was used to stain plasma membrane at a dilution of 1:1000 for 5-10 min prior to staining. Cells were washed in warm DMEM to remove excess stains. Warm Fluorbrite colorless DMEM was used for live cell imaging supplemented with 20 mM HEPES. For experiments involving phagocytosis of red fluorescent zymosan, zymosan was added at an MOI of 5 to cells prior to imaging. The imaging chamber was kept at 37°C. Images were obtained with a 40X oil immersion lens on a Zeiss confocal microscope. ASC-citrine signal was obtained with the green channel, MitoTracker Red CMXRos or red fluorescent zymosan in the red channel, and cell mask deep red in the infrared channel. Cells were identified as having visual ASC specks by the operator, and positions were logged. Automatic recall positions were visited over the course of 30 min for phagocytosis imaging assays to collect time-lapse movies. Videos were assembled side by side with indicator arrows added to identify specks using the video editing software iMovie.

Neon Electroporation

Electroporation was conducted using the Neon transfection machine, pipette, tips, and associated commercial buffers from ThermoFisher. For experiments involving electroporation of plasmid DNA into cells, 6E6 cells were suspended in 120 ul of R buffer from the Neon transfection kit. DNA was added to the cellular suspension at a concentration of 1.8 μg/1E6 cells. Cells were drawn into the neon transfection pipette and electroporated with the parameters of Voltage = 1150, pulse width = 20ms, and pulse number = 1.

Flow Cytometric Analysis of Electroporated Cells

IL-1β-tdTomato stable HEK293T cells were lifted with trypsin. Cells were counted and electroporated with GSDMD-EGFP fusion constructs as described above. For FACS experiments, ~6E5 electroporated cells were pipetted into FACS tubes in 0.5 mL of complete DMEM containing 5 mM glycine. When time points were taken, tubes were placed on ice and 7-AAD was added to assay for membrane permeability. Cellular debris from electroporation was excluded with FSC and SSC gating. EGFP, tdTomato, and 7-AAD fluorescence signals were recorded for cells at each time point on a FACS Canto II machine and analyzed with FlowJo v10.3.0.

Protein Expression and Purification

Full-length human gasdermin D (GSDMD) was cloned into pDB.His.MBP vector with a TEV cleavable N-teminal His_6.MBP tag using NdeI and Xho I restriction sites. To obtain full length GSDMD, *E. coli* BL21 (DE3) cells harboring pDB-His_6-MBP-GSDMD were grown in LB medium supplemented with 50 μg/ml kanamycin. Protein expression was induced overnight at 18°C with 0.5 mM isopropyl-B-D-thiogalactopyranoside (IPTG) after OD600 nm reached 0.8. Cells were harvested and resuspended in a lysis buffer containing 25 mM Tris-HCl (pH 8.0), 150 mM NaCl, 20 mM imidazole and 5 mM 2-mercaptoethanol, and homogenized by ultra-sonication. The cell lysate was clarified by centrifugation at 18,000 rpm at 4°C for 1 hr. The supernatant containing the target protein was incubated with Ni-NTA resin (QIAGEN) that was pre-equilibrated with the lysis buffer for 30 min at 4°C. After incubation, the resin-supernatant mixture was poured into a column and the resin was washed with the lysis buffer. The proteins were eluted by the lysis buffer supplemented with 500 mM imidazole. The His_6-MBP-tagged protein was further purified by HiTrap Q ion-exchange and Superdex G200 gel-filtration chromatography (GE Healthcare Life Sciences). The MBP tag was removed by overnight TEV protease digestion at 16°C. The cleaved protein was purified using HiTrap Q ion-exchange and Superdex 200 gel-filtration column.

Liposome Encapsulation, Pore-Dependent Release Assay, and Electron Microscopy

Phosphocholine (PC):phosphatidylserine (PS) liposomes were created by mixing PC and PS dissolved in chloroform in a glass test tube at a mass ratio of 3:2. Chloroform was evaporated by gentle application of a stream of inert nitrogen gas over the lipid solution in a chemical fume hood. Dried lipid film was resuspended in buffer containing 25 mM Tris-HCl (pH 8.0) and 150 mM NaCl to make a final concentration of lipid in solution of 5 μg/μl. 5 μg of recombinant protein IL-1β or IL-18 was incubated in 500 μL of reconstituted buffer / lipid solution. 10 μg of L-LDH isolated from rabbit muscle was incubated in 500 μL of reconstituted buffer / lipid solution. To increase reconstitution of dried lipid film with recombinant proteins and buffer, test tubes containing lipid, buffer, and recombinant proteins were covered in parafilm and incubated at 37°C for 10-15 min. The combined solution was then vortexed continuously for 5 min at room temperature to encapsulate recombinant proteins into large liposomes. The liposome solution was spun at 100,000 x g for 15 min at 4°C to pellet liposomes containing the recombinant protein. Supernatant containing the free protein was removed. The liposome pellet was gently washed 3 times with liposome buffer, resuspended in buffer, and then spun again at 100,000 x g for 15 min at 4°C to pellet liposomes containing recombinant protein. The liposome pellet was gently washed again 3 times with liposome buffer and resuspended in a final volume of 1200 μL for protein release experiments. 170 μL of the liposome solution were aliquoted into 7 ultracentrifuge tubes. One tube corresponding to the maximal pellet signal and minimal supernatant signal was spun at 100,000 x g for 30 min. The pellet was resuspended in the same volume of fresh liposome buffer as the harvested supernatant. 7.5 μg of recombinant caspase-11 was added to liposome solution aliquots for indicated time points. 22.5 μg of recombinant GSDMD was added to 200 μL of liposome solutions for indicated time points. Caspase-11 was thawed prior to experiments and left in the fridge for 24 hr to ensure optimal activity. GSDMD was thawed directly prior to experiments on the bench top at room temperature. For IL-1β or IL-18 experiments, 5X SDS buffer was added to resuspended pellet or harvested supernatants for subsequent western blotting. For LDH experiments, resuspended pellet was lysed with 10X lysis buffer from the Pierce LDH colorimetric quantification kit and liposome buffer to make a final volume equivalent to harvested supernatants. 50 μL of lysed pellet and supernatants were incubated with 50 μL of colormetric LDH substrate from the Pierce LDH quantification kit for 15-30 min to assay LDH activity. Absorbance was read at 490 nm and background at 680 nm to quantify LDH release from liposome experiments. Absorbance values were normalized using the mean of 3 technical replicates of lysed pellet set to 100% activity. All liposome release assays were repeated at least 3 times, and 4 batches of purified recombinant proteins were used with slight variation in potency noted between batches.

Fluorescent dextrans of differing molecular weights were resuspended in liposomes buffer containing 25 mM Tris-HCl (pH 8.0) and 150 mM NaCl to a concentration of 50 mg/ml. Liposomes were prepared by drying and resuspension in diluted dextran solutions at a final concentration of 25 mg/ml of dextrans with 5 mg/ml of total 3:2 PC:PS lipid. Maximum fluorescence was set to the lysed pellet of untreated equivalent aliquoted resuspended liposomes loaded with fluorescent dextrans where each MW of dextran was compared to its own lysed sample to account for loading and labeling variability between the different sizes.

For electron microscopy of PC:PS liposomes in the presence of recombinant proteins, copper grids coated with a layer of thin carbon were rendered hydrophilic immediately before use by glow-discharge in air with 25 mA current for 45 s. Liposome solutions were loaded onto the grids, air-dried for ~1 min and blotted, leaving a thin layer of sample on the grid surface. The grids were floated on a drop of staining solution containing 1.0% uranyl formate for 60 s. After air-drying, the grids were examined by the Tecnai G^2 Spirit BioTWIN electron microscope.

QUANTIFICATION AND STATISTICAL ANALYSIS

Statistical significance for experiments with more than two groups was tested with two-way ANOVA with Tukey multiple comparison test correction. Adjusted p values were calculated with Prism 7.0 from GraphPad and the designation of **** in the figures corresponds to a $p \leq 0.0001$. Data presented is representative of at least 3 independent repeats unless otherwise designated. Data with error bars are represented as mean ± SEM.